ENGINEERING MATHEMATICS

MSC 35X20 **DOI: 10.14529/jcem180401**

CRITICAL STATES OF THIN UNDERLAYERS UNDER TENSILE AFFORD

V. L. Dilman[1]**,** dilman49@mail.ru,
A. N. Dheyab[2]**,** aws.nth@gmail.com
[1] South Ural State University, Chelyabinsk, Russian Federation,
[2] Al-Mutanna Univirsity, Al-Mutanna, Republic of Iraq

Mathematical models of the stress state of plastic layers (interlayers) under the tensile load under plane deformation are investigated. The layer of rectangular shape is included in the strip of more durable material. The method of characteristics (slip lines) is used. The reasons that contact hardening is not fully realized are investigated. The characteristic fields in the layer in the process of loading are analyzed. The classification of characteristic fields at the critical moment of loading is given. The criterion for the full realization of contact hardening of the layer material is obtained. It depends on the relative thickness of the layer and the coefficient of mechanical heterogeneity of the joint. Explicit analytical expressions for calculating the critical load in the case of the full implementation of contact hardening are obtained.

Keywords: plastic layer; stress state; systems of nonlinear differential equations; contact hardening; coefficient of mechanical heterogeneity.

Introduction

Extensive literature is devoted to the study of the stress-strain state (SSS) and strength of thin plastic layers (interlayers) under the action of a tensile or compressive load. In one of the first papers devoted to the subject [1] an infinite plastic strip was considered. It can be taken as a model of a thin interlayer. It was noted in [1], that in this interlayer the tangential stresses do not vary along its length.

$$\partial\tau_{xy}/\partial x = 0. \tag{1}$$

Later on it was noted that this condition (the Prandtl hypothesis) can be adopted for simulation of the SSS of not very thin layers. From hypotheses related to stresses we can also note the hypothesis of linearity of tangential stresses of one of the variables [2–6]. Conditions (1) has a limited application. Nevertheless, there are meaningful papers [7–11], using, together with numerical methods, the condition (1). Various restrictions laid upon the classes of functions in which the solution is found, both of force and deformation nature, are given in [12, 13].

However, the features of strain state and the variety of critical states of thin plastic layers between the stronger sections of heterogeneous joints [6, 11–16] remain insufficiently studied. A more detailed theoretical understanding of the conditions for the manifestation of contact hardening and its effect on the strength of heterogeneous joints is also required.

The aim of the work is to explore mathematical models of the stress state of thin plastic layers depending on their mechanical and geometric parameters and, on this basis, to obtain conditions for the destruction of thin layers with the full implementation of contact hardening.

1. Critical States of the Joint

Let the tensile load increases in in the case under consideration. The material of the layer passes into a state of plastic flow in the process of loading. In other words, the loss of the plastic stability of the deformation process of the layer has occurred. However, in relatively thin layers, so-called ***contact hardening*** begins to appear at this time, requiring an increase in the external force for continuing the deformation to some point, which we call *a limiting state of the layer*. This state can also be called *a state of pre-destruction*, or ***a critical state*** in which the continuation of an increase in the external load leads to deformation of the layer with uncontrolled speed and rapid destruction.

SSS of a plastic body under a plane deformation is determined by five equations. In dimensionless variables, these equations take the following form [2]:

$$\frac{\partial \sigma_x}{\partial x} + \frac{\partial \tau_{xy}}{\partial y} = 0; \tag{2}$$

$$\frac{\partial \sigma_y}{\partial y} + \frac{\partial \tau_{xy}}{\partial x} = 0; \tag{3}$$

$$(\sigma_x - \sigma_y)^2 + 4\tau_{xy}^2 = 4; \tag{4}$$

$$\frac{\partial v_x}{\partial x} + \frac{\partial v_y}{\partial y} = 0; \tag{5}$$

$$\frac{\sigma_x - \sigma_y}{2\tau_{xy}} = \frac{\dfrac{\partial v_x}{\partial x} - \dfrac{\partial v_y}{\partial y}}{\dfrac{\partial v_x}{\partial y} + \dfrac{\partial v_y}{\partial x}}. \tag{6}$$

Here σ_x, σ_y and τ_{xy} – the stresses, ν_x, ν_y – the speed of movement in the appropriate directions. Equations (2) and (3) are the equations of equilibrium, (4) the plasticity condition, (5) the incompressibility equation, and (6) is the condition for the proportionality of stress deviates and strain rates.

All these equations are considered (Fig. 1) on a rectangle (rectangular section of the layer) of length 2 along the Ox axis and thickness $2\varkappa$, $\varkappa \in (0; 1)$ with the axes of symmetry as axes of the Cartesian coordinate system. Here $\varkappa$ is the relative thickness of the layer, i.e. the ratio of its thickness to length. The direction of the Oy axis coincides with the direction of the external load. On the coordinate axes, by virtue of symmetry, the tangential stresses are zero.

$$\tau_{xy}(x, 0) = \tau_{xy}(0, y) = 0. \tag{7}$$

On the free surface specified by the equation $x = 1$ it is assumed that there are no external loads:

$$\sigma_x(1, y) = 0; \quad \tau_{xy}(1, y) = 0. \tag{8}$$

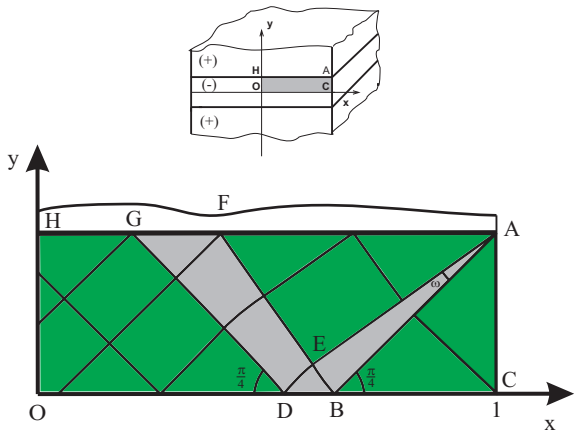

Fig. 1. A cross-section of a less hard layer in a heterogeneous joint and a field of characteristics (slip lines) at an early stage of its plastic deformation

Proceeding from symmetry, it is sufficient to consider a quarter of the layer $x \geq 0, y \geq 0$ (rectangle $OHAC$ in Fig. 1).

The system of equations (2) – (4) is closed (three equations and three unknown functions σ_x, σ_y и τ_{xy}) and, together with conditions (7) and (8), determines the stress state of the plastic layer.

At the moment of the transition of the layer from the elastic to the plastic state, its stress field is homogeneous: at all points of the layer in dimensionless values

$$\sigma_x = 0; \quad \sigma_y = 2; \quad \tau_{xy} = 0. \tag{9}$$

Both families set of characteristics of a homogeneous field are families of lines. As the tensile load increases, homogeneous field (9) is distorted. Areas of a fan-centered field appear in the form of circular sectors with vertices at the corner points of the layer (Fig. 1 and 2, section EAB). The change in the stress state of the layer is seen as an increase from zero of the angles ω^- of these sectors. We will call the section of the field *simple* if one of its families of characteristics is rectilinear.

Further transformation of the field of slip lines (characteristics) and the form of this field depends on the loading stage and the two main connection parameters: $\varkappa$ and K – *the coefficient of mechanical heterogeneity of the joint*. The form of the field of characteristics in the critical state of the layer, including the magnitude of the angle ω^-, is completely determined by parameters $\varkappa$ and K. One of the possible patterns of the characteristics field at an intermediate moment is shown in Fig. 2. Here the triangles ABC and AEF and the quadrilateral $DOHG$ are sections of the uniform field of characteristics, sector ABE and area $DGFE$ are sections of a simple field, area BDE is covered by curvilinear characteristics.

At first the basic material is deformed elastically during the process of increasing the external load. As the load increases, angle ω^- increases too, and point D moves to point O. There are several possible situations for the deformation process of the stretchable joint, accompanied by an increase in the contact hardening of the layer.

Situation 1. In the process of increasing the external load, angle ω^- reaches the theoretically possible maximum:

$$\omega^- = \pi/4 \tag{10}$$

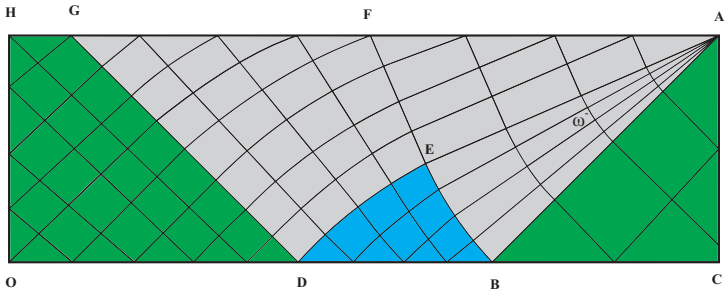

Fig. 2. The field of characteristics (slip lines) in the intermediate stage of loading of the plastic layer, $\varkappa = 0{,}32$

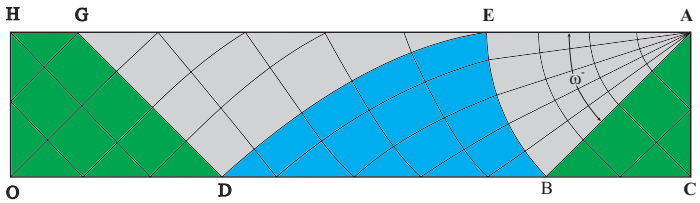

Fig. 3. The field of characteristics (slip lines) in the intermediate stage of loading of the plastic layer with full realization of contact hardening, $\varkappa = 0{,}21$

(Fig. 3), whereas point D does not reach point O. In this case the basic material does not go anywhere in the state of plasticity. On the segment EA, the tangential stresses reach their absolute maximum: $\tilde{\tau}_{xy} = k^-$, or, in dimensionless values $\tau_{xy} = 1$. In Fig. 3, contact hardening has not yet reached its limit. Indeed, the field of characteristics can continue to vary so that, even outside the segment, the tangential stresses can turn out to be equal to 1 (more fully about this in the next section).

Thus, condition (10) is equivalent to the equality of the tangential stresses to one in a certain segment LA including EA (Fig. 3). When segment LA reaches its greatest possible value, the so-called ***full realization of contact hardening*** takes place. In [12, pp. 81–83], the system of equations determining the conjugation conditions of normal and tangential stresses on the contact surface was numerically solved. On this basis, it was shown there that inequality

$$K \geq K_{cr} \approx 1{,}98 \tag{11}$$

is necessary to satisfy condition (10). For small values $\varkappa$, condition (11) can be sufficient to satisfy condition (10). We shall call such layers ***thin underlayers***.

Situation 2. As angle $EAB = \omega^-$ increases, point D (Fig. 1–3) of characteristic AED moves to the axis of symmetry of the layer – axis Oy, i.e. to point O. The extreme position in this situation is the hit of characteristic AED in the center of the layer, i.e. to the coincidence of the points D and O. At this moment, angle ω^- turned out to be smaller $\pi/4$, and its further increase contradicts to condition (7). Under such conditions, further deformation of the field of characteristics and, as a consequence, growth of contact hardening cease. The reason for this phenomenon is the "too large" relative thickness of the layer. In the terminology of O.A. Bakshi, there is an incomplete implementation of contact hardening. We must note that in not very thin interlayers, contact hardening

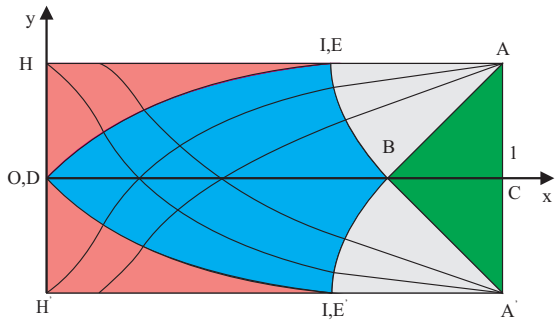

Fig. 4. The field of characteristics of the plastic layer of the smallest relative thickness $\varkappa = 0{,}251$ subject to the full implementation of contact hardening. Characteristic AED falls into layer center O

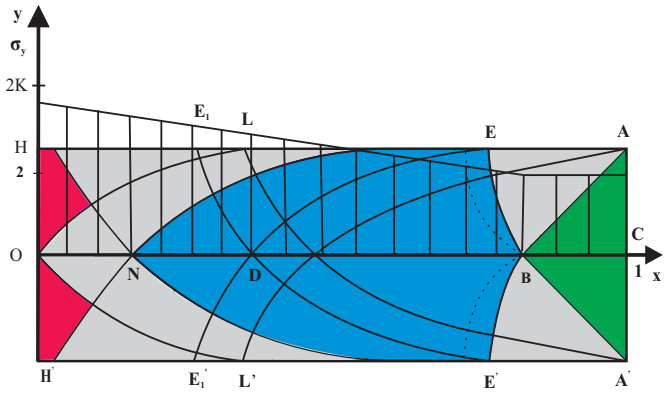

Fig. 5. The field of characteristics of a thin less hard layer provided the full implementation of the contact hardening at the critical moment of loading, when $\varkappa = 0{,}178$, and the stress diagram σ_y along the axis of symmetry of the layer (the first type of the stress state of the layer)

is not fully realized even under condition (11). The lower boundary $\varkappa^*$ of the relative thickness of such interlayers will be calculated below. The boundary case between two marked situations arises when, at the moment of the coincidence of points D and O, angle ω^- is equal to $\pi/4$ (Fig. 4).

The stress state of the layer at the critical moment of loading also depends on whether normal stresses σ_y in some part of the layer reach stresses $2K$ in the basic part of the material. We call *the first type of the critical state of the layer* the case when $\sigma_y < 2K$ everywhere in the layer (Fig. 5) and *the second type of critical state of the layer* – when at some part of the layer $\sigma_y = 2K$ (see the section HNH' in Fig. 6 and the section $HMNM'H'$ in Fig. 7). Note that if the angle between the contact and free surfaces is not equal to $\pi/2$, then the value of K_{cr} depends on this angle.

Situation 3. With the growth of the external load, there may be a moment when the process of deformation of the layer ceases, in spite of the fact that point D has not reached point O, and angle $\omega^- < \pi/4$. This occurs when the basic material in the near-boundary zone goes plastic state. Then the further increase of angle ω^- stops 1, the contact

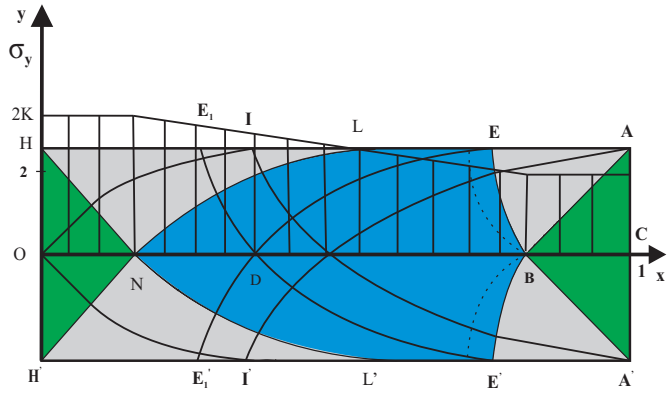

Fig. 6. The field of characteristics of a thin less hard layer provided the full implementation of the contact hardening at the critical moment of loading, when $\varkappa = 0{,}158$, and the stress diagram σ_y along the axis of symmetry of the layer (the second type of the stress state of the layer)

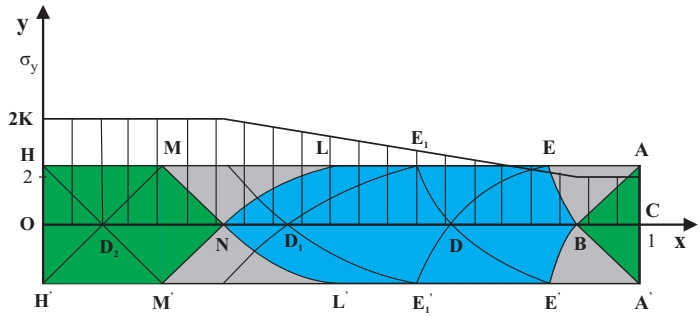

Fig. 7. The field of characteristics of a thin less hard layer provided the full implementation of the contact hardening at the critical moment of loading, when $\varkappa = 0{,}088$, and the stress diagram σ_y along the axis of symmetry of the layer (the second type of the stress state of the layer)

hardening has reached the limiting value and, as in situation 2, is not fully realized. This phenomenon occurs when the mechanical heterogeneity is not very considerable [6, 13–16].

2. Conditions for the Full Implementation of Contact Hardening

The stress state of a loaded solid at each point is related to its field of characteristics by well-known relationships. If the external load acts in the direction of axis Oy with plane deformation, the following dependences take place:

$$\begin{cases} \sigma_x &= \sigma - \sin 2\gamma; \\ \sigma_y &= \sigma + \sin 2\gamma; \\ \tau_{xy} &= \cos 2\gamma. \end{cases} \tag{12}$$

Here γ is the angle of inclination of the characteristics to axis Ox.

Let us consider a thin interlayer in situation 1, when condition (10) is satisfied. The effect of the basic part of the joint on a less durable layer leads to an increase in tangential

stresses on the contact surface. On segment EA (Fig. 4), in the limiting state, the tangential stresses reach their maximum value:

$$\tau_{xy}^{-}(x, \varkappa) = 1, \tag{13}$$

which in view of last equation (12) $\tau_{xy} = \cos 2\gamma$ is equivalent to condition: $\gamma = 0$. Suppose that the tangential stresses are maximal also on the segment LE adjacent to EA. Then the characteristics along LE touch contact line HA. Let LA be the largest segment on the contact boundary, where $\tau_{xy}^{-} = 1$. Note that $H \neq L$, since $\gamma_H = \pi/4$. The tangential stresses on axis Ox are indeed zero for symmetry reasons.

Such stress state arises in particular under Prandtl condition of the constancy of tangential stresses along the layer:

$$\partial\tau_{xy}/\partial x = 0.$$

For the layers symmetric with respect to axis Ox for which $\tau_{xy}(x, 0) = 0$ this condition is obviously equivalent to the following equality:

$$\tau_{xy} = y/a \tag{14}$$

for some constant a.

It is common knowledge [2] that the slip lines (characteristics) are arcs of the cycloid under L.Prandtl's condition. The zone in which this condition at least approximately occurs, forms area $OLEBE'L'$ at the cross-section of the layer (Fig. 5). The form of the characteristic field in Fig. 5 is approximate. In some vicinities of curves EB and OL – the boundaries of the Prandtl area – the stressed state has an intermediate form, not being exactly Prandtl's. For example, the curve EB can not be both an arc of a circle and a cycloid at the same time. Cycloids passing through point B are shown in phantom in Fig. 5.

If section LE is absent, then the zone of the Prandtl stresses is a quadrangle $OEBE'$ in Fig. 7. The layer shown in this Figure is the thickest (broadest) of all layers, in which at point E the characteristic touches the contact line. This is equivalent to (13), in view of the last equation (12). Let us find the relative thickness $\varkappa$ of such layer, assuming that in the section $DEBE'$ (Fig. 7), there occurs Prandtl stress state. Let us calculate the coordinates of points D and E_1. In view of the above assumption and formulas (12) and (14) for points of curve DE, the following assumptions are satisfied:

$$\begin{cases} \tau_{xy} &= \cos 2\gamma, \\ \tau_{xy} &= y/a. \end{cases}$$

Hence follows the equation of the characteristic in the Prandtl zone as a function of the ordinate of the tilt angle of the characteristic:

$$y = a \cos 2\gamma. \tag{15}$$

At point E the tangent to curve DE is horizontal, i.e. $\gamma_E = 0$. Obviously $y_E = \varkappa$, therefore

$$a = \varkappa. \tag{16}$$

We find the equation of the curve DE as a function x of γ. From .. It follows from (15) and (16) that $y = \varkappa \cos 2\gamma$.. Therefore

$$\frac{dx}{d\gamma} = \frac{dx}{dy}\frac{dy}{d\gamma} = \varkappa \operatorname{tg}^{-1}\gamma(\cos 2\gamma)' = -4\varkappa \cos^2\gamma,$$

from which we find the equation of the curve DE:

$$x = -\varkappa(2\gamma + \sin 2\gamma + C).$$

Substituting the coordinates of the point E: $\gamma_E = 0$, $x_E = 1 - \sqrt{2}\varkappa$ in the previous equation, we get the value of the constant C. The equation of the curve DE has the form:

$$x = -\varkappa(2\gamma + \sin 2\gamma) + 1 - \sqrt{2}\varkappa. \tag{17}$$

Since at point D $\gamma_D = \pi/4$, from (17) we get:

$$x_D = -\varkappa(\pi/2 + 1) + 1 - \sqrt{2}\varkappa. \tag{18}$$

Obviously, $x_B = 1 - \varkappa$. Therefore

$$|DB| = x_B - x_D = (\pi/2 + \sqrt{2})\varkappa. \tag{19}$$

Consequently, the relative thickness of the thickest layer, which allows a complete realization of contact hardening, is equal to

$$\varkappa = \frac{|AC|}{|OC|} = \frac{|AC|}{|OB| + |BC|} = \frac{\varkappa}{(\pi/2 + \sqrt{2})\varkappa + \varkappa} = \frac{1}{1 + \pi/2 + \sqrt{2}} \approx 0{,}251.$$

Let us call a less hard layer *a thin (thin interlayer)* if its relative thickness

$$\varkappa \le \varkappa^*, \quad \varkappa^* = \frac{1}{1 + \pi/2 + \sqrt{2}} \approx 0{,}251. \tag{20}$$

Summarizing the results, we obtain:

Proposition 1. *For the full realization of contact hardening, it is necessary and sufficient that two conditions be satisfied: (10) and (20).*

The characteristics grid for the boundary case $\varkappa = \varkappa^*$ is shown in Fig. 7.

To obtain the dimensions of Prandtl zone let us calculate $|E_1D|$. On the curve E_1D $\gamma_{E_1} = -\pi/2$, $y_{E_1} = \varkappa$. Substituting these values into (15), we get: $a = -\varkappa$. Since it is obvious that

$$\frac{dy}{dx} = -ctg\gamma,$$

from (15) it follows that

$$\frac{dx}{d\gamma} = \frac{dx}{dy}\frac{dy}{d\gamma} = \varkappa \operatorname{tg}\gamma \frac{dy}{d\gamma} = \varkappa \operatorname{tg}\gamma \frac{d\cos 2\gamma}{d\gamma} = -4\varkappa \sin^2\gamma.$$

Therefore, the equation of the curve E_1D can be written in the form:

$$x = -4\varkappa \int \sin^2\gamma \, d\gamma = -\varkappa(2\gamma - \sin 2\gamma + C).$$

Since $\gamma_D = -\pi/4$, and x_D is calculated by formula (18), we get the abscissa of point E_1:

$$x_{E_1} = -\pi\varkappa + 1 - \sqrt{2}\varkappa.$$

And finally,

$$|E_1D| = x_{E_1} - x_D = \varkappa(\pi/2 - 1) \approx 0{,}57\varkappa.$$

3. The Critical State of the Less Hard Layer Provided the Full Implementation of the Contact Hardening

The average critical stress in the stretching of a homogeneous strip in dimensionless coordinates is equal to the value of

$$\sigma_{cr} = 2K.$$

Since at all points of the layer the critical normal stress can not exceed the stress at the corresponding point of a homogeneous strip of more durable material, there is an inequality for all points of a less strong layer:

$$\sigma_y(x, y) \le 2K. \tag{21}$$

The stress state of the layer under the Prandtl condition is well known [2, 5]:

$$\begin{cases} \sigma_x(x, y) &= -x/a - 2\sqrt{1 - y^2/a^2} + C; \\ \sigma_y(x, y) &= -x/a + C; \\ \tau_{xy}(x, y) &= y/a, \end{cases} \tag{22}$$

where in view of (16) $a = \varkappa$, and constant C to be defined. To find it, we note that on the one hand $\sigma_x(B) = -x_B/a - 2 + C$ by the first formula (22), and on the other hand, $\sigma_x(B) = 0$. Consequently $C = 1/\varkappa + 1$. Therefore

$$\sigma_y(x, y) = -x/\varkappa + 1/\varkappa + 1 \tag{23}$$

in view of (22).

Let us consider two types of stress state of a layer.

The first type of stress state of the layer. Let the condition (21) be satisfied throughout the layer (see Fig. 5). Then the Prandtl stress state takes place in the region containing entire segment OB of axis Ox. It follows the implementation of inequalities from the conditions (21) and (20):

$$\frac{1}{2K - 1} \le \varkappa \le \varkappa^* \approx 0{,}251. \tag{24}$$

The set of values $\varkappa$ at which the (24) is executed is not empty provided

$$K \ge \frac{\varkappa^* + 1}{2\varkappa^*} \approx 2{,}5. \tag{25}$$

Proposition 2. *The first type of stress state is realized if and only if (24) and (25). The average critical effort is calculated by the formula:*

$$\sigma_{cr} = \frac{(\varkappa + 1)^2}{2\varkappa}. \tag{26}$$

Proof.

Using (23), we obtain:

$$\sigma_{cr} = \int_0^1 \sigma_y(x, 0)\, dx = \int_0^{1-\varkappa} \left(\frac{1 - x}{\varkappa} + 1 \right) dx + 2\varkappa = \frac{(\varkappa + 1)^2}{2\varkappa}.$$

□

The second type of stress state of the layer. Let on some segment $[0; N]$ of axis Ox stress $\sigma(x, y)$ calculated by formula (22) exceed $2K$ on some segment $[0; N]$ of axis Ox. This means that for some point N of axis Ox the formula is incorrect on the segment ON, and stresses $\sigma_y(x, y) = 2K$ (see Fig. 6 and Fig. 7). Such conditions arise if

$$\begin{cases} \varkappa(2K-1) \le 1; \\ K \ge K_{cr} \approx 1,98; \\ \varkappa \le \varkappa^* \approx 0{,}251. \end{cases} \tag{27}$$

This type of stress state is determined by the following field characteristics (see Fig. 6 and 7). In the area $OHMNM'H'$ the field is simple homogeneous. In triangles NML and $N'M'L'$ the field is transitional between Prandtl field and homogeneous field, where one of two sets of characteristics consists of straight lines.

Coordinate x_N of point N is found from equation $\sigma(x, y) = 2K$, which gives in view of (23):

$$x_N = 1 + \varkappa - 2\varkappa K. \tag{28}$$

Proposition 3. *The second type of stress state is realized if and only if (27). The average critical effort is calculated by the formula:*

$$\sigma_{cr} = 2K(1 + \varkappa - \varkappa K). \tag{29}$$

Proof.

$$\sigma_{cr} = \int_0^1 \sigma_y(x, 0)\, dx = \int_0^{x_N} 2K\, dx + \int_{x_N}^{1-\varkappa} \left(\frac{1-x}{\varkappa} + 1 \right) dx + 2\varkappa.$$

Using (23), we obtain:

$$\int_0^{x_N} 2K\, dx = 2K + 2\varkappa K - 4\varkappa K^2, \quad \int_{x_N}^{1-\varkappa} \left(\frac{1-x}{\varkappa} + 1 \right) dx = 2\varkappa K^2 - 2\varkappa.$$

Hence follows (29).

□

Both types of stress state of the layer occur in the intermediate case $\varkappa(2K-1) = 1$. Then the formulas (26) and (29) coincide.

References

1. Prandtl L. Beispiele der Anwendung des Hencky's Theorems zum Gleichgewicht der plastischen Körper. *Z. Angew. Math. Mech.*, 1923, vol. 3, no. 6, pp. 401–406. DOI: 10.1002/zamm.19230030601.

2. Kachanov L. M. *Fundamentals of the Theory of Plasticity.* Amsterdam, North-Holland Publishing Company, 1971.

3. Kachanov L. M. On the Stress State of a Plastic Interlayer. *Izv. AN SSSR. OTN. Mekhanika i Mashinostroenie*, 1962, no. 5, pp. 63–67. (in Russian).

4. Satoh K., Toyoda M. Joint Strength of Heavy Plastics with Lower Strength Weld Metal. *Welding Journal*, 1975, issue 9, pp. 311–319.

5. Unksov E. P. [Once Again About the Flat Sediment of a Strip Between Parallel Rough Plates]. *Kuznechno-pressovoe Proizvodstvo – Press Forging*, 1980, no. 5, pp. 18–20. (in Russian).

6. Ostsemin A. A., Dil'man V. L., Compression of a Plastic Layer by Two Rough Plates. *Strength of Materials*, 1990, vol. 22, no. 7, pp. 1076–1085. DOI: 10.1007/BF00767561.

7. Kim Y.-J., Schwalbe K.-H. Numerical Analysis of Strength Mis-match Effect on Local Stresses for Ideally Plastic Material. *Engineering Fracture Mechanics*, 2004, vol. 71, issue 7–8, pp. 1177-1199. DOI: 10.1016/S0013-7944(03)00141-3.

8. Schnabl S., Saje M., Turk G., Planinc I. Analytical Solution of Two-Layer Beam Taking into Account Interlayer Slip and Shear Deformation. *Journal of Structural Engineering*, 2007, vol. 133, no. 6, pp. 886–894. DOI: 10.1061/(ASCE)0733-9445(2007)133:6(886).

9. Kozak D., Gubeljak N., Konjatić P., Sertić J. Yield Load Solutions of Heterogeneous Welded Joints. *International Journal of Pressure Vessels and Piping*, 2009, vol. 86, issue 12, pp. 807–812. DOI: 10.1016/j.ijpvp.2009.11.012.

10. Alexandrov S., Harris D. Geometry of Principal Stress Trajectories for a Mohr-Coulomb Material under Plane Strain. *Zeitschrift für Angewandte Mathematik und Mechanik*, 2017, vol. 97, no. 4, pp. 473–476. DOI: 10.1002/zamm.201500284.

11. Alexandrov S., Kuo C.Y., Jeng Y.R. A Numerical Method for Determining the Strain Rate Intensity Factor under Plane Strain Conditions. *Continuum Mechanics and Thermodynamics*, 2015, vol. 28, no. 4, pp. 977–992. DOI: 10.1007/s00161-015-0436-3.

12. Dilman V. L., Eroshkina T. V. *Mathematical Modelling of Critical States of the Soft Layers in Heterogeneous Joints*. Chelyabinsk, Publishing Center of SUSU, 2011. (in Russian).

13. Dilman V. L. *Mathematical Modes of Stress States of Heterogeneous Thin-walled Cylindrical Shells*. Chelyabinsk, Publishing Center of SUSU, 2007. (in Russian).

14. Dil'man V. L., Ostsemin A. A. Effect of Stress Concentration in a Welded Seam on the Low-Cycle Fatigue of Large-Diameter Pipes. *Chemical and Petroleum Engineering*, 2003, vol. 39, issue 5–6, pp. 259–264.

15. Dilman V. L., Karpeta T. V. The Stress State of a Plastic Layer with a Variable Yield Strength under a Flat Deformation, *Russian Mathematics (Iz. VUZ)*, 2013, vol. 57, issue 8, pp. 29–36. DOI: 10.3103/S1066369X13080045.

16. Dil'man V. L., Ostsemin A. A. Analysis of the Ductile Strength of Welds Weakened by Notches in Longitudinally Welded Pipes of Large Diameter by the Method of Slip Lines, *Strength of Materials*, 2004, vol. 36, issue 3, pp. 274–281. DOI: 10.1023/B:STOM.0000035761.47001.4c.

Valery L. Dilman, DSc (Math), Head of Department of Mathematical Analysis and Methods of Teaching Mathematics, South Ural State University (Chelyabinsk, Russian Federation), dilman49@mail.ru.

Aws N. Dheyab, Middle-Professor of Department of Mathematics and Computer Technology, Al-Mutanna Univirsity (Al-Mutanna, Republic of Iraq), aws.nth@gmail.com.

Received November 1, 2018.

УДК 539.4 **DOI: 10.14529/jcem180401**

КРИТИЧЕСКИЕ СОСТОЯНИЯ ТОНКИХ ПРОСЛОЕК ПОД РАСТЯГИВАЮЩЕЙ НАГРУЗКОЙ

В. Л. Дильман, А. Н. Дияб

Исследуются математические модели напряженного состояния пластических слоев (прослоек) под растягивающей нагрузкой при плоской деформации. Прослойка прямоугольной формы входит в состав полосы из более прочного материала. Используется метод характеристик (линий скольжения). Исследованы причины неполной реализации контактного упрочнения. Проанализированы поля характеристик в слое в процессе нагружения. Дана классификация полей характеристик в критический момент нагружения. Получен критерий полной реализации контактного упрочнения материала прослойки в зависимости от относительной толщины прослойки и коэффициента механической неоднородности соединения. Получены явные аналитические выражения для вычисления критической нагрузки при полной реализации контактного упрочнения.

Ключевые слова: пластический слой; напряженное состояние; системы нелинейных дифференциальных уравнений; контактное упрочнение; коэффициент механической неоднородности.

Литература

1. Prandtl, L. Beispiele der Anwendung des Hencky's Theorems zum Gleichgewicht der plastischen Körper / L. Prandtl // Z. Angew. Math. Mech. – 1923. – V. 3, № 6. – P. 401–406.
2. Kachanov, L. M. Fundamentals of the Theory of Plasticity / L. M. Kachanov. – Amsterdam: North-Holland Publishing Company, 1971.
3. Качанов, Л. М. О напряженном состоянии пластичной прослойки / Л. М. Качанов // Изв. АН СССР. Отд. техн. наук. Механика и машиностроение. – 1962. – № 5. – С. 63–67.
4. Satoh, K. Joint Strength of Heavy Plastics with Lower Strength Weld Metal / K. Satoh, M. Toyoda // Welding Journal. – 1975. – Iss. 9. – P. 311–319.
5. Унксов, Е. П. Еще раз о плоской осадке полосы между параллельными шероховатыми плитами / Е. П. Унксов // Кузнечно-прессовое производство. – 1980. – № 5. – С. 18–20.

6. Ostsemin, A. A. Compression of a Plastic Layer by Two Rough Plates / A. A. Ostsemin, V. L. Dil'man // Strength of Materials. – 1990. – V. 22, № 7. – P. 1076–1085.
7. Kim, Y.-J. Numerical Analysis of Strength Mis-match Effect on Local Stresses for Ideally Plastic Material / Y.-J. Kim, K.-H. Schwalbe // Engineering Fracture Mechanics. – 2004. –V. 71, iss. 7–8. – P. 1177–1199.
8. Schnabl, S. Analytic Solution of Analytical Solution of Two-Layer Beam Taking into Account Interlayer Slip and Shear Deformation / S. Schnabl, M. Saje, G. Turk, I. Planinc // Journal of Structural Engineering. – 2007. – V. 133, № 6. – P. 886–894.
9. Kozak, D. Yield Load Solutions of Heterogeneous Welded Joints / D. Kozak, N. Gubeljak, P. Konjatić, J. Sertić // International Journal of Pressure Vessels and Piping. – 2009. – V. 86, iss. 12. – P. 807–812.
10. Alexandrov, S. Geometry of Principal Stress Trajectories for a Mohr-Coulomb Material under Plane Strain / S. Alexandrov, D. Harris // Zeitschrift für Angewandte Mathematik und Mechanik. – 2017. – V. 97, № 4. – P. 473–476.
11. Alexandrov, S. A Numerical Method for Determining the Strain Rate Intensity Factor under Plane Strain Conditions / S. Alexandrov, C. Y. Kuo, Y. R. Jeng // Continuum Mechanics and Thermodynamics. – 2015. – V. 28, № 4. – P. 977–992.
12. Дильман, В. Л. Математическое моделирование критических состояний мягких прослоек в неоднородных соединениях / В. Л. Дильман, Т. В. Ерошкина. – Челябинск: Издат. центр ЮУрГУ, 2011.
13. Дильман, В. Л. Математические модели напряженных состояний неоднородных тонкостенных цилиндрических оболочек / В. Л. Дильман. – Челябинск: Издат. центр ЮУрГУ, 2007.
14. Дильман, В. Л. Напряженное состояние и прочность сварных соединений труб большого диаметра / В. Л. Дильман, А. А. Остсемин // Химическое и нефтегазовое машиностроение. – 1998. – № 4. – С. 16–20.
15. Дильман, В. Л. Напряженное состояние пластического слоя с переменным по толщине пределом текучести при плоской деформации / В. Л. Дильман, Т. В. Карпета // Изв. вузов. Матем. – 2013. – № 8. – С. 34–43.
16. Dil'man, V. L. Analysis of the Ductile Strength of Welds Weakened by Notches in Longitudinally Welded Pipes of Large Diameter by the Method of Slip Lines / V. L. Dil'man, A. A. Ostsemin // Strength of Materials. – 2004. – V. 36, iss. 3. – P. 274–281.

Дильман Валерий Лейзерович, доктор физико-математических наук, заведующий кафедрой математического анализа и методики преподавания математики, Южно-Уральский государственный университет (г. Челябинск, Российская Федерация), dilman49@mail.ru.

Дияб Аус Нидал, преподаватель кафедры математики и компьютерных технологий, Университет Ал-Мутанны (Ал-Мутанна, Республика Ирак), aws.nth@gmail.com.

Поступила в редакцию 1 ноября 2018 г.